N O T I C E

THIS DOCUMENT HAS BEEN REPRODUCED FROM MICROFICHE. ALTHOUGH IT IS RECOGNIZED THAT CERTAIN PORTIONS ARE ILLEGIBLE, IT IS BEING RELEASED IN THE INTEREST OF MAKING AVAILABLE AS MUCH INFORMATION AS POSSIBLE

NASA Technical Memorandum 79282

ADHESION, FRICTION, AND WEAR OF
BINARY ALLOYS IN CONTACT WITH
SINGLE-CRYSTAL SILICON CARBIDE

Kazuhisa Miyoshi and Donald H. Buckley
Lewis Research Center
Cleveland, Ohio
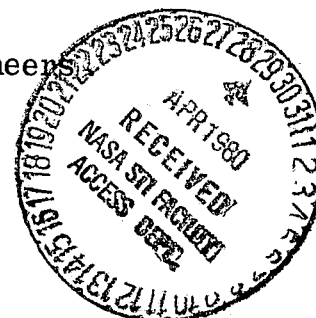
ADHESION, FRICTION, AND WEAR OF BINARY ALLOYS IN CONTACT WITH SINGLE-CRYSTAL SILICON CARBIDE

by Kazuhisa Miyoshi and Donald H. Buckley

ABSTRACT

Sliding friction experiments were conducted with various iron-base alloys (alloying elements were Ti, Cr, Mn, Ni, Rh, and W) in contact with a single-crystal silicon carbide {0001} surface in vacuum. Results indicate atomic size misfit and concentration of alloying elements play a dominant role in controlling adhesion, friction, and wear properties of iron-base binary alloys. The controlling mechanism of the alloy properties is as an intrinsic effect involving the resistance to shear fracture of cohesive bonding in the alloy. The coefficient of friction generally increases with an increase in solute concentration. The coefficient of friction increases as the solute-to-iron atomic radius ratio increases or decreases from unity. Alloys having higher solute concentration produce more transfer to silicon carbide than do alloys having low solute concentrations. The chemical activity of the alloying element is also an important parameter in controlling adhesion and friction of alloys.

INTRODUCTION

Silicon carbide is widely used as an abrasive for industrial grinding. However, because the surface interactions involved are so complex, our knowledge of the industrial grinding is limited. A better understanding of the fundamental behavior of silicon carbide during the process of grinding should alter improvements in its efficiency by providing a more judicious selection of materials, lubricants, and operating parameters.

Fundamental studies on the surface interactions, that is, the friction and wear behavior of silicon carbide should commence with clean surfaces of comparatively simple, pure metals and binary or ternary alloys.

The present authors have conducted experimental studies to determine the tribological properties of single-crystal silicon carbide in contact with clean surfaces of pure metals in vacuum (ref. 1). It is very important to gain a better fundamental understanding of tribological properties of silicon carbide sliding against alloys. Because it is well known that the presence of small amounts of alloying elements in alloyed metals can markedly alter their surface activity (refs. 2 to 4). The authors also found that small concentrations of chromium in iron resulted in an increase in the adhesion and friction of the alloys contacting silicon carbide (ref. 5). The exact role of alloying elements in the adhesion, friction, and wear of alloy-ceramic contacts was not clearly revealed in reference 5, because of the small selection of alloying elements.

On the other hand, the atomic size and concentration of the alloying element are extremely important for the abrasive-wear and friction behavior of iron-base binary alloys in contact with silicon carbide. The coefficient

of friction and abrasive wear volume generally decreases with increasing solute concentration (ref. 6). There is a correlation between the solute-to-solvent (iron) atomic radius ratio and the coefficient of friction. There is also a good relation between wear and the change in solute concentration. Friction and wear decrease as the solute-to-iron atomic radius ratio either increases or decreases from unity. Thus, of further interest are the effects of atomic size and concentration of alloying element on the adhesive wear and friction of alloys.

This investigation was conducted to determine the effect of alloying elements (such as Ti, Cr, Mn, Ni, Rh, and W) on the adhesion, friction and wear behavior of iron-base, binary, solid-solution alloys in sliding contact with single-crystal silicon carbide {0001} surface. Experiments were conducted with loads of 0.05 to 0.3 newton, at a sliding velocity of 3×10^{-3} meter per minute, in a vacuum of 10^{-8} pascal, at room temperature with sliding on the silicon carbide {0001} basal plane in the $\langle10\bar{1}0\rangle$ direction. The alloys were all polycrystalline.

MATERIALS

Table I presents the analyzed compositions in atomic percent of the iron-base alloys used in the present investigation. The iron-base binary alloys were prepared by Stephens and Witzke (ref. 7), and they arc-melted the high-purity iron and high-purity alloying elements (Ti, Cr, Mn, Ni, Rh, and W). The solute concentrations ranged from approximately 0.5 atomic percent for these elements that have extremely limited solubility in iron up to approximately 16 atomic percent for these elements that form a series of solid solutions with iron.

The single-crystal silicon carbide used in these experiments was a 99.9-percent-pure compound of silicon and carbon and had a hexagonal-closed packed crystal structure. The composition and microhardness data, of single-crystal silicon carbide are also shown in table II.

EXPERIMENTAL APPARATUS AND PROCEDURE

Apparatus

The apparatus used in the investigation was mounted in an ultrahigh vacuum system. The apparatus measures adhesion, load, and friction. The vacuum system also contained tools for surface analysis, an Auger emission spectrometer (AES), and a low-energy electron diffraction (LEED) system. The mechanism used for measuring adhesion, load, and friction is shown schematically in Fig. 1. A gimbal-mounted beam is projected into the vacuum system. The beam contains two flats machined normal to each other with two strain gages mounted thereon. The 0.79-millimeter radius alloy pin is mounted on the end of the beam. As a load is applied by moving the beam in the direction normal to the disk, it is measured by the strain gage. The vertical sliding motion of the pin along the disk surface is accomplished through a motorized gimbal assembly. Under an applied load the friction force is measured during vertical translation of the strain gage mounted

2

normal to that used to measure load. This feature was used to examine the coefficient of friction at various loads, as shown in Fig. 1.

Specimen Preparation

The iron-base binary alloy pins and the disks of silicon carbide were polished with 3-micrometer-diameter diamond powder and then 1-micrometer-diameter aluminum oxide (Al_2O_3) powder. Both pin and disk surfaces were rinsed with 200-proof ethyl alcohol before installation in the vacuum chamber.

The specimens were then placed in the vacuum chamber, which was evacuated and baked out to a pressure of 1.33×10^{-8} pascal (10^{-10} torr). And then, argon gas was bled back into the vacuum chamber to a pressure of 1.3 pascals. A 1000-volt-direct-current potential was applied, and the specimens (both disk and pin) were argon sputter bombarded for 30 minutes. After sputtering was completed, the vacuum chamber was reevacuated, and AES (Auger emission spectroscopy) spectra of the disk surface were obtained to determine the degree of surface cleanliness. When the disks were clean, as evidenced by Auger spectra, friction experiments were conducted.

Experimental Procedure

Loads of 0.05 to 0.3 newton were applied to the pin-disk contact by deflecting the beam of Fig. 1. Both load and friction force were continuously monitored during the friction experiments. The sliding velocity was 3 millimeters per minute, with a sliding distance of 2.5 millimeters per pass sliding. All friction experiments in vacuum were conducted with the system evacuated to a pressure of 10^{-8} pascal.

RESULTS AND DISCUSSION

Cleanliness of Silicon Carbide Surfaces

An Auger emission spectroscopy spectrum of the single-crystal silicon carbide {0001} surfaces obtained before sputter cleaning, but after polishing and bake out is shown in figure 2(a). In addition to the silicon and carbon peaks, an oxygen peak is also present. The oxygen peak and the chemically shifted silicon peaks at 78 and 89 electron volts (eV) indicate a layer of SiO_2 on the silicon carbide surfaces as well as a simple, adsorbed film of oxygen (refs. 8 and 9). The Auger spectrum taken after the silicon carbide surface had been sputter cleaned (fig. 2(b)) clearly reveals the silicon and carbon peaks at 92 and 272 eV, respectively; the oxygen peak is negligible.

Fundamental Behavior of Adhesion, Friction, and Wear

<u>Adhesion and friction</u>. - Sliding friction experiments were conducted with iron-base binary alloys in contact with single-crystal silicon carbide in vacuum. The binary alloy systems were iron alloyed with various concentration with titanium, chromium, manganese, nickel, rhodium or tungsten.

Figure 3 shows typical friction-force traces resulting from such slidings. The friction-force traces obtained in this investigation are characterized by a sharp break in the friction force at point b in Fig. 3, that is, stick-slip behavior. The line a-b in Fig. 3 represents the region where both loading and tangential (shear) forces are being applied, but where no gross sliding occurred. The point b is the onset of slip. Line b-c represents the region where the surfaces of alloy and silicon carbide are in rapid slip. In Fig. 3(b), the points c may be located at the same place as a.

The coefficient of static friction μ_s is defined: $\mu_s = F_{max}/W$, where F_{max} is the friction force at which the first sharp break is observed in the friction force trace and W is the normal load.

The average coefficient of friction μ in a single pass sliding or multi-pass sliding is defined as: $\mu = \overline{F}_{max}/W$, where $\overline{F}_{max}$ is the average friction force calculated from maximum-peak-heights in which the sharp breaks are observed in the friction force trace.

Wear. - Figure 4 represents a scanning electron micrograph and an X-ray map of a wear track on the silicon carbide generated by a single stick and slip of the 8.12 atomic percent titanium-iron alloy rider, as shown in Fig. 3(a). In the X-ray energy dispersive map, the concentrations of white spots correspond to those locations in the micrograph (fig. 4(b)), where copious amounts of alloy have transferred. It is obvious from those photographs that a large amount of alloy transfers to the silicon carbide surface. In Fig. 4(a) the light area, where a lot of alloy transfer is evident, was the contact area before sliding of the rider. It is the area where the surfaces of alloy and silicon carbide were sticking to one to the other and where strong interfacial adhesion occurred. This area, where both the loading and tangential (shear) force were applied to the specimen, corresponds with the region a-b of Fig. 3(a). All of the single-crystal silicon carbide surfaces in sliding contact with the alloys shown in table I contained the metallic elements on their surfaces, indicating transfer of the alloy to silicon carbide with even a first single stick and slip of the alloy rider on silicon carbide.

Figure 5 represents typical rider wear scar on an iron-base binary alloy (in this case, 8.12 at % Ti-Fe alloy) generated by a single stick and slip behavior as shown in Fig. 3(a). The size of wear scar is comparable with that of the area of alloy transfer shown in Fig. 4. The wear scars reveal a large number of small size grooves and microcracks formed primarily by shearings of the interfaces and in the bulk of the alloys. Close examination of Fig. 5(b) indicates that the cracks are very small in size, are in the wear scar, and propagate nearly perpendicular to the sliding direction.

Figure 6 represents scanning electron micrographs of a wear track on the silicon carbide surface and a wear scar of the alloy rider generated by 10 passes of the alloy on silicon carbide. It becomes obvious from Fig. 6(a) that the copious amount of alloy transfer to the silicon carbide occurs with multi-contact and sliding. Alloys, generally, produced four types of wear with alloy multi-pass sliding on silicon carbide: (1) a very thin

transfer film on the contact area, (2) multilayer transfer films, (3) very small particles (submicron in size), and (4) piled-up particles (several micrometers in size). The transfer film is observed in the wear track on silicon carbide surface. The particles are seen in and by the wear track. This result is consistent with earlier study (ref. 1).

The wear scars on all the alloy riders after they slid against silicon carbide showed evidence of (1) a large number of plasticity deformed grooves, indentations, and cracks. The grooves and indentations were the result of plowing by transferred alloy debris on silicon carbide, and/or sliding and rolling of wear debris of silicon carbide and alloy. The cracks, as typically shown in Fig. 7, propagate perpendicular to the sliding direction in the wear scar of the alloy. Such cracks initiate and propagate with maximum shear stresses in the weakest interfacial region of alloy in the process where both loading and tangential forces are being applied to the interface.

Thus, fracture of cohesive bonds in alloy occurs during sliding. And the shearing at the interface and in the bulk are the main factors responsible for the observed adhesion, friction and wear behavior.

Effects of alloying element on the tribological behavior will be discussed in the next section.

Alloying Element Effects on Tribological Properties

Adhesion and friction. - The coefficients of friction for a number of iron-base binary alloys in contact with silicon carbide were examined as a function of load. All examinations indicated no significant change in the coefficient of static friction or the average coefficient of friction during single pass sliding with load over the load range of 0.05 to 0.3 newton.

The average coefficients of static friction over the entire load range for iron-base binary alloys are presented in Fig. 8 as a function of solute concentration. The data of these figures indicate that the coefficient of friction generally increases markedly with the presence of any alloying element relative to the results for pure iron. This continues with further increases in the concentration of alloying element but not so markedly as the initial increase. The increasing rate in the coefficient of friction strongly depends on the alloying element.

It should be noted that the average coefficient of friction for pure iron in sliding contact with single-crystal silicon carbide was about 0.5 (ref. 1). This value was obtained under identical experimental conditions to those of this investigation. The coefficient of friction was about 0.6 for pure titanium, 0.5 for pure nickel and tungsten and 0.4 for pure rhodium. The coefficients of friction for the alloys are generally much higher, as much as twice those for pure metals.

Figure 9 presents the average coefficients of static friction for the various alloys of Fig. 9 as a function of solute-to-iron atomic radius

5

ratio. In Fig. 9(a), the solute concentrations are all about 4 atomic percent. In Fig. 9(b) the coefficients of static friction for the maximum solute concentration (see table I) of each are plotted. The maximum solute concentrations extend to approximately 16 atomic percent.

There appears to be good agreement between the adhesion and friction and the solute-to-iron atomic radius ratio. The correlation of the coefficient of static friction and solute-to-iron atomic radius ratio is separated into two cases: first, the case for alloying with manganese and nickel, which have smaller atomic radii than iron; and, second, the case for alloying with chromium, rhodium, tungsten, and titanium, which have larger atomic radii than iron. The coefficients of static friction increase generally as the solute-to-iron atomic radius ratio increases or decreases from unity. The increasing rate of the coefficients of static friction for alloying elements, that have smaller atomic radii than iron are much greater than that for alloying elements, that have larger atomic radii than iron. Atomic size ratio values reported herein are from Ref. 7. The correlations indicate that the atomic size of the solute is an important factor in controlling the adhesion and friction in iron-base binary alloys as well as the abrasive wear and friction reported by the present authors (ref. 6) and the alloy hardening reported by Stephens and Witzke (ref. 7). The controlling mechanism of adhesion and friction of alloys may be raising the Peierles stress and/or an increase in lattice friction stress, by solute atoms, resisting the shear fracture of cohesive bonding in the alloy.

More detailed examination of Fig. 9 indicates that the correlation for manganese, nickel, and chromium is better than that for titanium, tungsten, rhodium, and chromium. The coefficient of friction for rhodium is relatively low, and that for titanium is relatively high. The relative chemical activity of the transition metals (metals with partially filled d shell) as a group can be ascertained from their percent d bond character after Pauling (ref. 10). The authors already determined that the coefficient of friction for silicon carbide in contact with various transition metals was related to the d bond character, that is, chemical activity of the metal (ref. 1). The more active the metal, the higher the coefficient of friction. Table III shows the reciprocal d bond character of metals calculated from the data of Ref. 10. The greater the reciprocal percent d bond character, the more active the metal and the higher the coefficient of friction (ref. 1).

Rhodium-iron alloys in contact with silicon carbide showed relatively low friction. On the other hand, titanium-iron alloys showed relatively high friction. The results seem to be related to the chemical activity of alloying elements, that is, the rhodium is less active and titanium is more active, as indicated in table III. The good correlation for manganese, nickel and chromium in Fig. 9 is due to the reciprocal percent d bond character for those being the almost same value for each.

Wear and friction. - The transfer of the alloy to silicon carbide had occurred with a single pass sliding of the alloy rider to silicon carbide. Once the transfer of alloy starts in the first single-pass sliding of the rider, the phenomenon of multi-pass slidings becomes one of alloy sliding

6

against itself or both alloy and silicon carbide. This influences subsequent friction properties and alloy transfer to the silicon carbide and the nature of transfer film. And it is anticipated that the friction properties and alloy transfer will be related to the alloy element and its concentration.

Figure 10 represents typical data of the coefficients of friction as a function of number of passes. When repeated passes of the alloy riders are made over the same single-crystal silicon carbide surface, the coefficients of friction for alloys having high solute concentration or chemically active alloying elements (Mn, Ni, Ti) in table I generally decreased with number of passes. The coefficients of friction for first pass sliding differ much from those for the second pass sliding and multiple pass sliding. This is due to a large amount of alloy transfer to the silicon carbide surface even in the first single-pass sliding of the rider.

On the other hand, the coefficients of friction for the alloy having low solute concentration or chemically less active alloying element generally exhibit small changes and fluctuations with the number of passes, as is shown typically in Fig. 10(b).

The fluctuating behavior of the coefficient of friction also strongly depends on the nature of the transfer of the alloys.

For iron-base binary alloys with solutes such as titanium, tungsten, chromium, nickel and manganese, the coefficients of friction during multipass sliding generally decrease as the solute concentration increases. Alloys having high solute concentration in table I produced much more transfer than do alloys having low solute concentration, as was already mentioned in a former section. These phenomena of friction and alloy transfer are consistent. The phenomenon of multipass sliding for alloy having high solute concentration is strongly becoming one of alloy sliding against itself rather than against silicon carbide. That for alloy having low solute concentration become alloy sliding against both alloy and silicon carbide.

Thus, the friction properties in multipass sliding strongly depend on the amount and nature of alloy transfer which is controlled by the alloying element and its concentration. Therefore, examination of changes in the coefficient of friction with number of passes will suggest a measure of the amount or nature of alloy transfer.

Figure 11 presents changing of coefficient of friction with number of passes as a function of solute concentrations at a load of 0.2 newton. The changes were estimated from the data, and are shown typically in Fig. 10. The changing of coefficient of friction is expressed as: $\mu_1 - \mu_{multipass} = \Delta\mu$. Where μ_1 is the coefficient of friction for first pass sliding and $\mu_{multipass}$ is the average coefficient of friction calculated from the coefficients of friction for second to tenth-pass slidings. The change of coefficient of friction generally increases as the solute concentration increases with the exceptions of rhodium and chromium and

the change of coefficient of friction strongly depends on the alloying element.

Therefore, those changes were plotted as a function of material, that is, the solute-to-iron atomic radius ratio in Fig. 12. There appears to be very good agreement between the change of coefficient of friction with number of passes and the solute to iron atomic radius ratio. The correlation between the rate and the solute to iron atomic radius ratio is separated into two cases: first, the case for alloying with manganese and nickel, which have smaller atomic radii from iron, and second, the case for chromium, rhodium, tungsten, and titanium, which have larger atomic radii than iron. The change $\Delta\mu$ or $\Delta\mu/\mu_1$ increases as the solute to iron atomic radius ratio increases or decreases from unity.

Thus, the correlation in Fig. 12 indicates that atomic size of the solute is an important measure in the change of the coefficient of friction, and the amount and nature of alloy transfer during multipass sliding.

CONCLUSIONS

The following conclusions are drawn from the data presented herein:

1. The atomic size misfit and the concentration of alloying element are important factors in controlling the adhesion and friction of iron-base, binary alloy in contact with silicon carbide.

2. The controlling mechanism of adhesion and friction of alloys can be raising the Peierles stress and/or an increase in lattice friction stress by solute atoms, resisting the shear fracture of cohesive bonding in the alloy.

3. The coefficient of friction generally increases markedly with the presence of any concentration of alloying element in the pure metal and more gradually with increasing the concentration of alloying element.

4. The coefficients of friction generally increase as the solute-to-iron atomic radius ratio increases or decreases from unity.

5. The atomic size misfit and the concentration of alloying element are factors in controlling the friction and alloy transfer to silicon carbide during multipass slidings.

Alloys having high solute concentration produce more transfer than do alloys having low solute concentrations. The change of coefficient of friction during multipass sliding, which is influenced by alloy transfer, increases as the solute-to-iron atomic radius ratio increases or decreases from unity.

REFERENCES

1. Miyoshi, K. and Buckley, D. H., "Friction and Wear Behavior of Single-Crystal Silicon Carbide in Sliding Contact with Various Metals," ASLE Transactions, Vol. 22, No. 3, 1979, pp. 245-256.

2. Jordan, L. K.; and Scheibner, E. J., "Characteristic Energy Loss Spectra of Copper Crystals with Surfaces Described by LEED," Surface Science, Vol. 10, 1968, pp. 373-391.

3. Evans, D. R. and Flanagan, W. F., "Solid-Solution Strengthening of Face Centered Cubic Alloys," Philosophical Magazine, Vol. 18, No. 155, Nov., 1968, pp. 977-983.

4. Buckley, D. H., "A LEED Study of the Adhesion of Gold to Copper and Copper-Aluminum Alloys," NASA TN D-5351, 1969.

5. Miyoshi, K. and Buckley, D. H., "Friction and Wear Characteristics of Iron-Chromium Alloys in Contact with Themselves and Silicon Carbide," NASA TP-1387, 1979.

6. Miyoshi, K. and Buckley, D. H., "The Friction and Wear of Metals and Binary Alloys in Contact with an Abrasive Grit of Single-Crystal Silicon Carbide," ASLE Preprint No. 79-LC-5C-1, Oct. 1979.

7. Stephens, J. R. and Witzke, W. R., "Alloy Softening in Binary Iron Solid Solutions," Journal of the Less-Common Metals, Vol. 48, Aug., 1976, pp. 285-308.

8. Johannessen, J. S., Spicer, W. E., and Strausser, Y. E., "An Auger Analysis of the SiO_2-Si Interface," Journal of Applied Physics, Vol. 47, No. 7, July 1976, pp. 3028-3037.

9. Miyoshi, K. and Buckley, D. H., "Effect of Oxygen and Nitrogen Interactions on Friction of Single-Crystal Silicon Carbide," NASA TP-1265, 1978.

10. Pauling, L., "A Resonating-Valence-Bond Theory of Metals and Intermetallic Compounds," Proceedings of the Royal Society (London), Seri. A, Vol. 196, No. 1046, Apr. 7, 1949, pp. 343-362.

TABLE I – CHEMICAL ANALYSIS[a] AND SOLUTE TO IRON ATOMIC RADIUS RATIOS

FOR IRON-BASE BINARY ALLOYS

Solute element	Analyzed solute content, at. %	Analyzed interstitial content, ppm by weight			Solute to iron atomic radius ratios (b)
		C	O	P	
Ti	1.02	56	92	7	1.1476
	2.08	--	---	--	
	3.86	87	94	9	
	8.12	--	---	--	
Cr	0.99	--	---	--	1.0063
	1.98	50	30	12	
	3.92	--	---	--	
	7.77	40	85	10	
	16.2	--	---	--	
Mn	0.49	--	---	--	0.9434
	.96	39	65	6	
	1.96	--	---	--	
	3.93	32	134	8	
	7.59	--	---	--	
Ni	0.51	--	---	--	0.9780
	1.03	28	90	6	
	2.10	--	---	--	
	4.02	48	24	5	
	8.02	--	---	--	
	15.7	38	49	7	
Rh	1.31	--	---	--	1.0557
	2.01	20	175	22	
	4.18	--	---	--	
	8.06	12	133	19	
W	0.83	30	140	12	1.1052
	1.32	--	---	--	
	3.46	23	61	21	
	6.66	--	---	--	

[a]Reference 3.

[b]References 10 and 3 and "table of periodic properties of the elements," published by L. L. Wymon and J. J. Park from National Bureau of Standards, USCOMM-DC-28,801, 1961.

TABLE II – COMPOSITION DATA, CRYSTAL STRUCTURE, AND

HARDNESS OF SINGLE-CRYSTAL SILICON CARBIDE

(a) Composition[a]

Si	C	O	B	P	Others
66.6%	33.3%	<500 ppm	<100 ppm	<200 ppm	<0.1 ppm

(b) Structure

Interatomic distance		Lattice ratio, c/a
a	c	
3.0817	15.1183	4.9058
3.073	15.079	4.9069

(c) Hardness data

Plane	Direction	Knoop hardness number (2.9 N)
(0001)	$<11\bar{2}0>$	2670
(0001)	$<10\bar{1}0>$	2825

[a] Manufacturer's analyses.

TABLE III – AMOUNT AND RECIPROCAL OF d CHARACTER FOR TRANSITION ELEMENTS

Metal	Fe	Mn	Ni	Cr	Rh	W	Ti
Amount of d character	39.7	40.1	40.0	39	50	43	27
Reciprocal d character	0.68	0.67	0.68	0.69	0.54	0.63	1

SLIDING

DISK SPECIMEN

HEMISPHERICAL PIN (RIDER)

LOAD

GIMBAL

TRANSLATIONAL MOTION

ADHESIVE FORCE

FRICTION FORCE
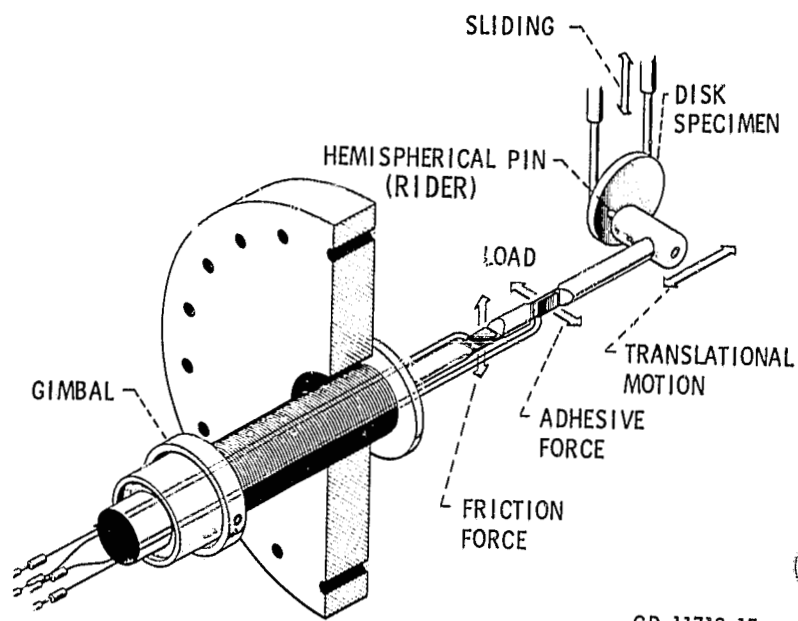
CD-11718-15

Figure 1. - High-vacuum friction and wear apparatus.

(a) BEFORE SPUTTER CLEANING.

(b) AFTER SPUTTER CLEANING.
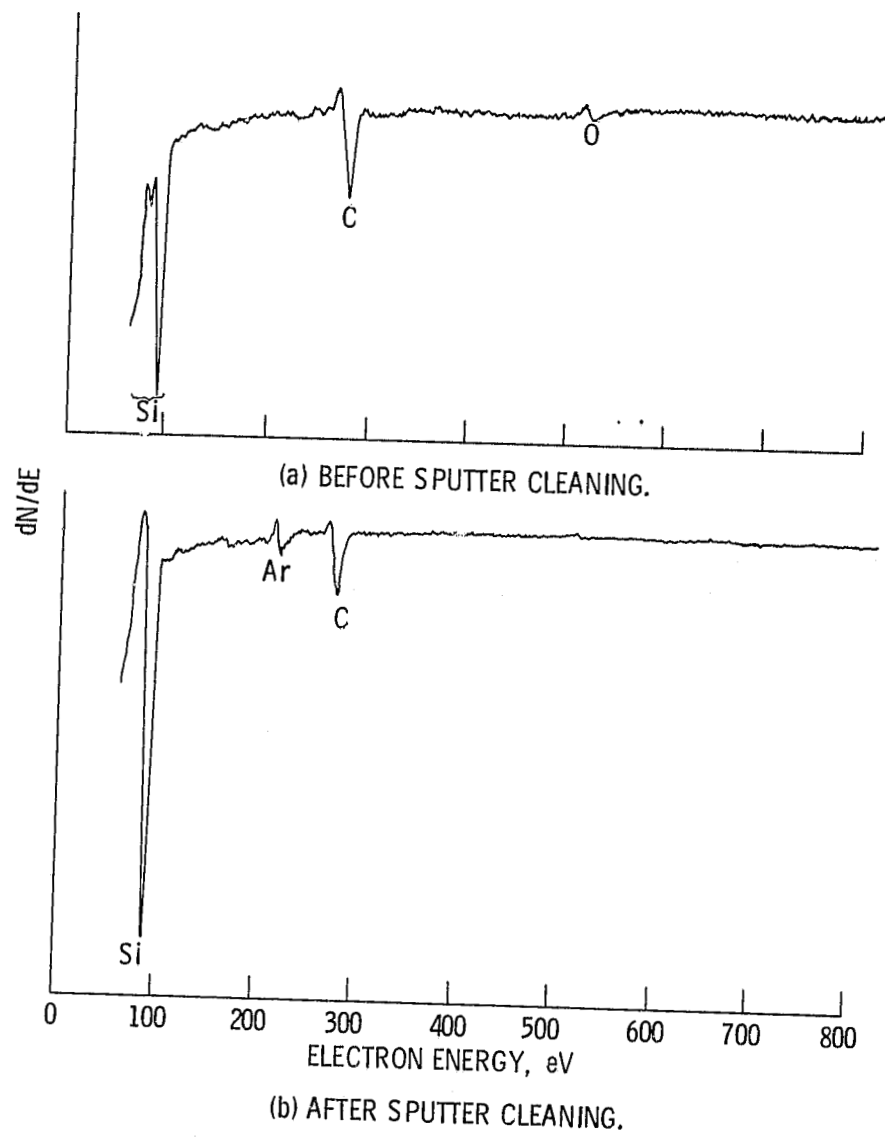
Figure 2. - Auger spectra of single-crystal silicon carbide (0001) surface.
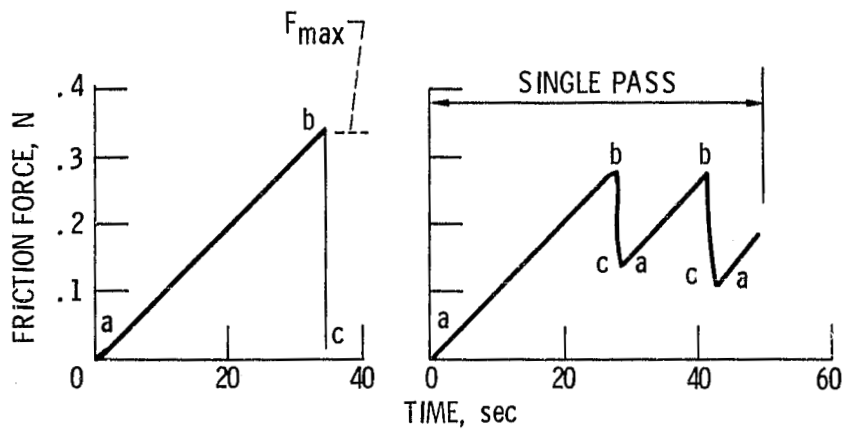
(a) FIRST STICK AND SLIP.

(b) SINGLE PASS SLIDING (AT 10 PASSES SLIDING).

Figure 3. – Typical examples of friction force trace for 8.12 at.% Ti-Fe alloy sliding on single-crystal silicon carbide {0001} surface. Load, 0.2 N.

SLIDING
DIRECTION
OF RIDER

ALLOY TRANSFER

10 μm

(a) SCANNING ELECTRON MICROGRAPH.

10 μm
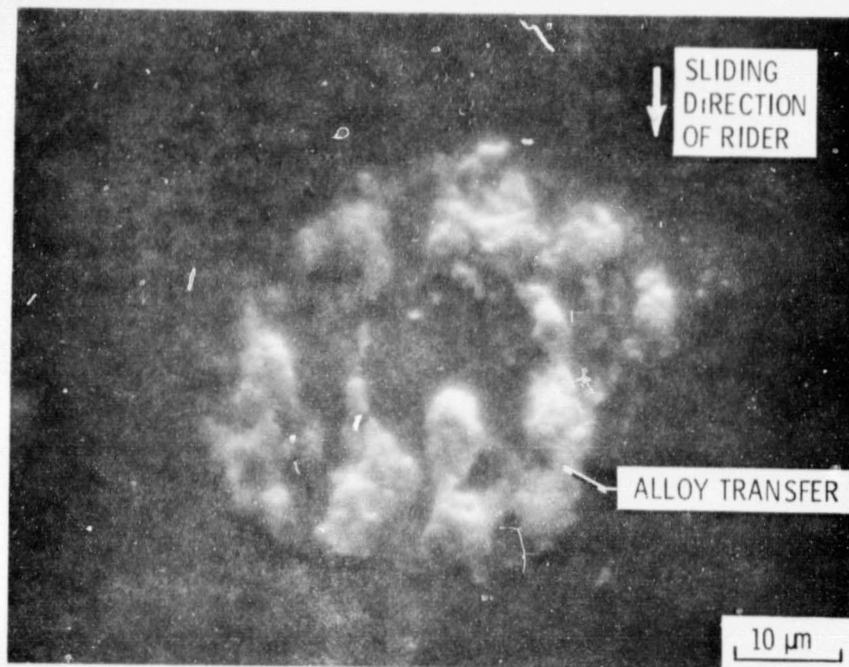
(b) IRON Kα, X-RAY MAP (5000 COUNTS).

Figure 4. - Titanium-iron binary alloy (8.12 at. % Ti) transfer to single-crystal silicon carbide (0001) surface at start of sliding. Silicon carbide (0001) surface; sliding direction $\langle 10\bar{1}0 \rangle$; sliding velocity, 3 mm/min; load, 0.2 N; room temperature; vacuum pressure, 10^{-8} Pa.
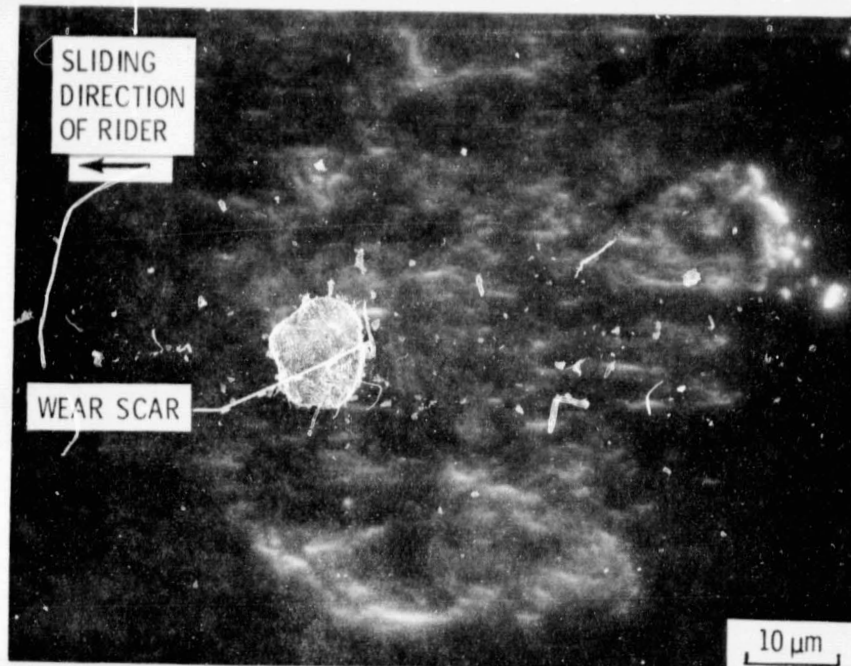
(a) LOW MAGNIFICATION.
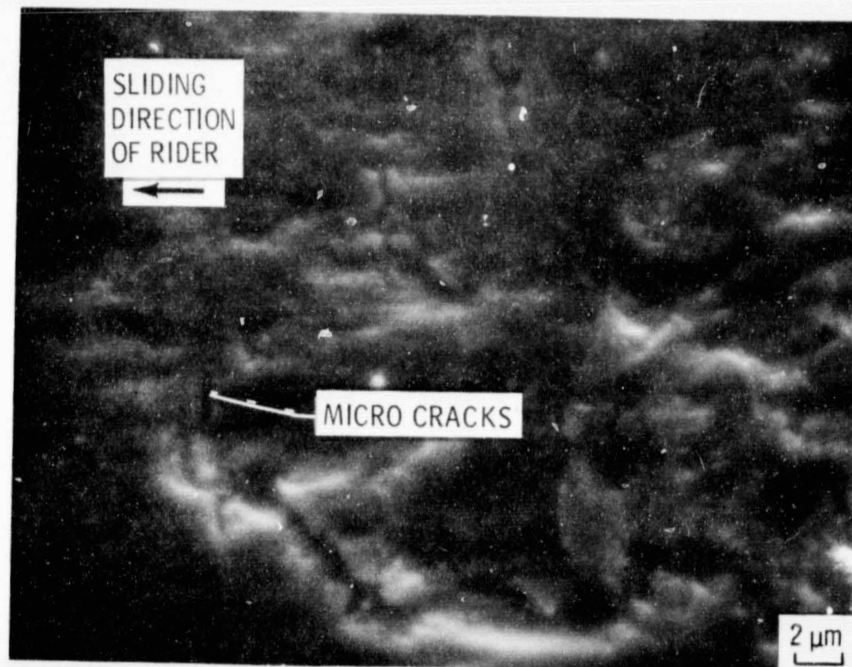
(b) HIGH MAGNIFICATION.

Figure 5. - Wear scar on titanium-iron binary alloy (8.12 at. % Ti) rider showing grooves and cracks. Single pass on SiC (0001) surface; sliding direction $\langle 10\bar{1}0 \rangle$; sliding velocity, 3 mm/min; load, 0.2 N; room temperature; vacuum pressure, 10^{-8} Pa.
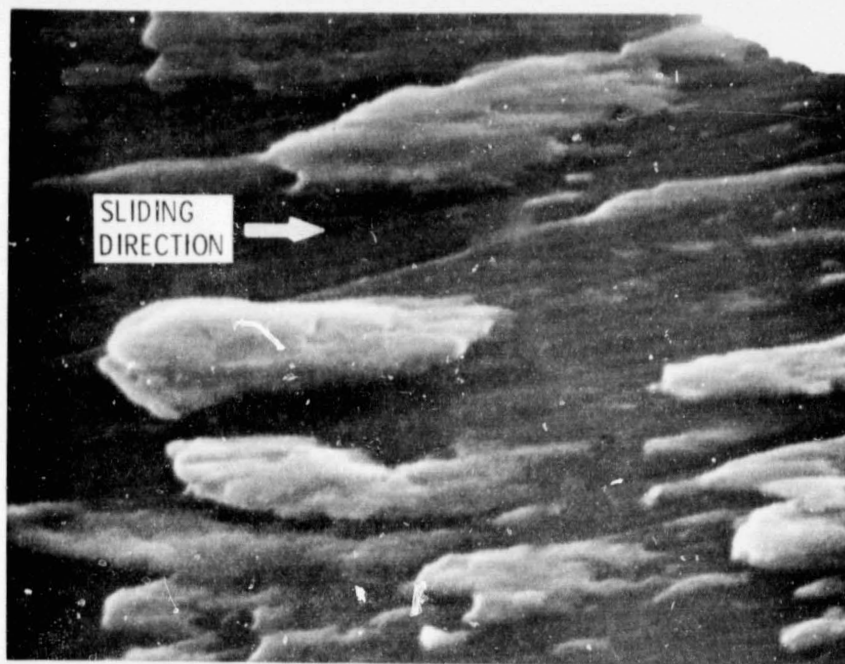
(a) 8. 12 at. % Ti-Fe ALLOY TRANSFER.

(b) 2. 68 at. % Ti-Fe ALLOY TRANSFER.

Figure 6. - Ti-Fe alloys transferred to single-crystal silicon carbide during sliding as a result of 10 passes of riders. Scanning electron micrographs of wear tracks on silicon carbide {0001} surfaces during sliding. Load, 0.2 N.

SLIDING
DIRECTION

10 μm

(a) SCANNING ELECTRON MICROGRAPH.

SLIDING
DIRECTION

5 μm
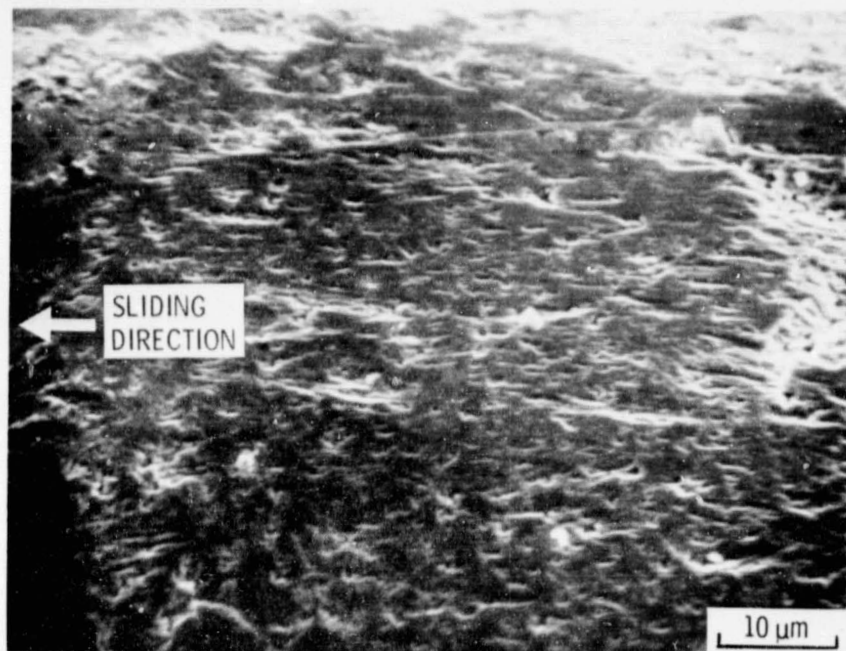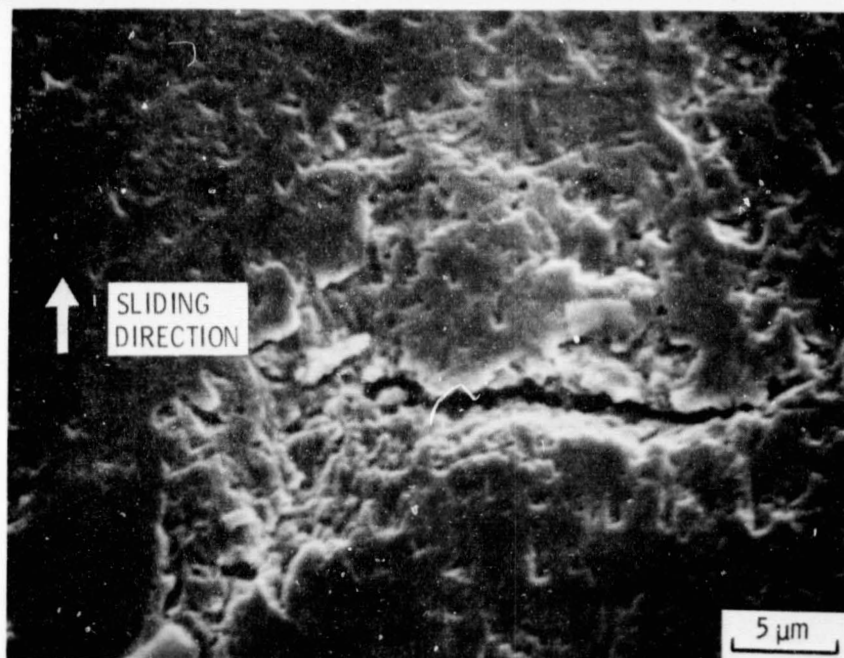
(b) SCANNING ELECTRON MICROGRAPH.

Figure 7. - Wear scar on 8.12 at. % Ti-Fe alloy rider showing grooves,
indentations, and fracture. Ten passes on silicon carbide {0001}
surface; load, 0.2 N.
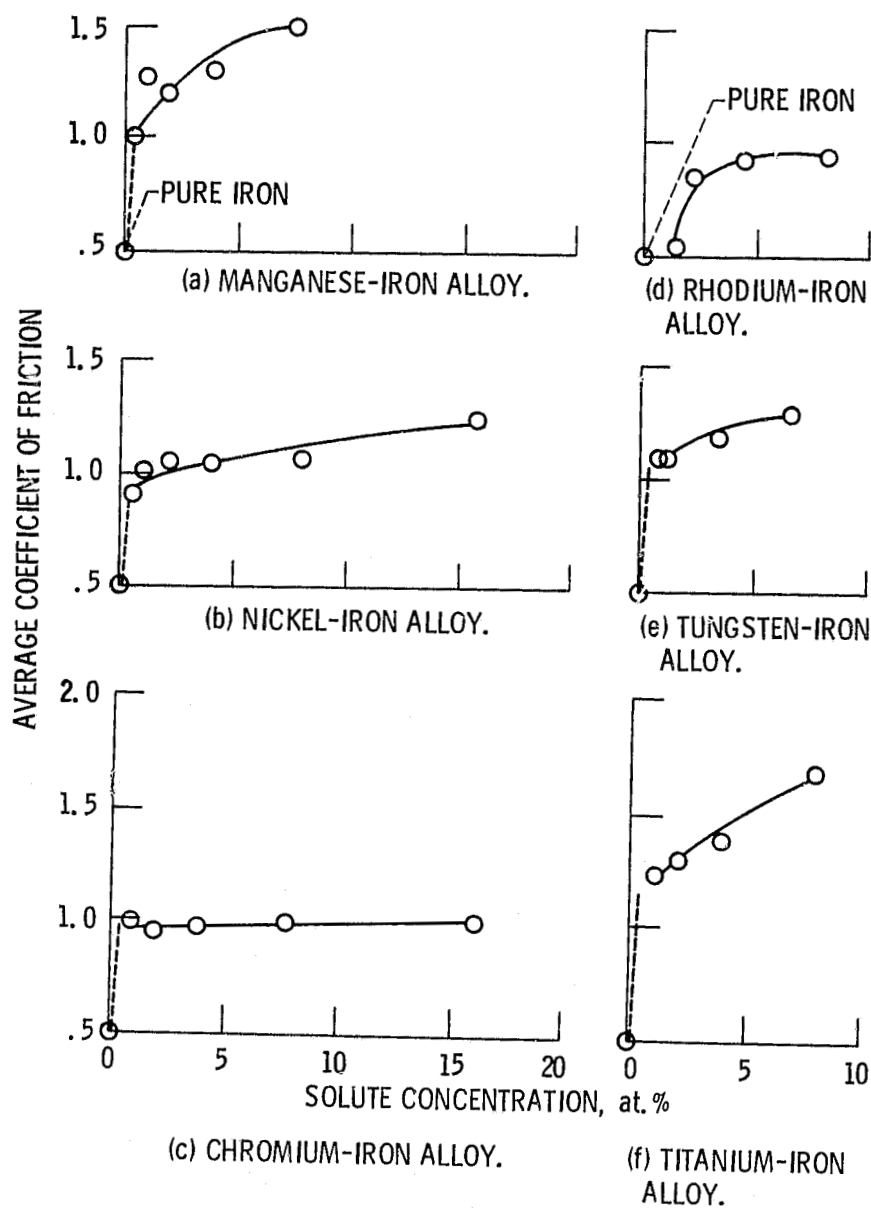
Figure 8. - Coefficient of friction for various iron-base binary alloys as function of solute concentration. Single-pass sliding on single-crystal silicon carbide (0001) surface; sliding direction, $\langle 10\bar{1}0 \rangle$; sliding velocity, 3 mm/min; load, 0.2 N; room temperature; vacuum pressure, 10^{-8} Pa.

(a) Solute concentration of about 4 at. %.

(b) Maximum solute concentrations of alloys. (See table I.)
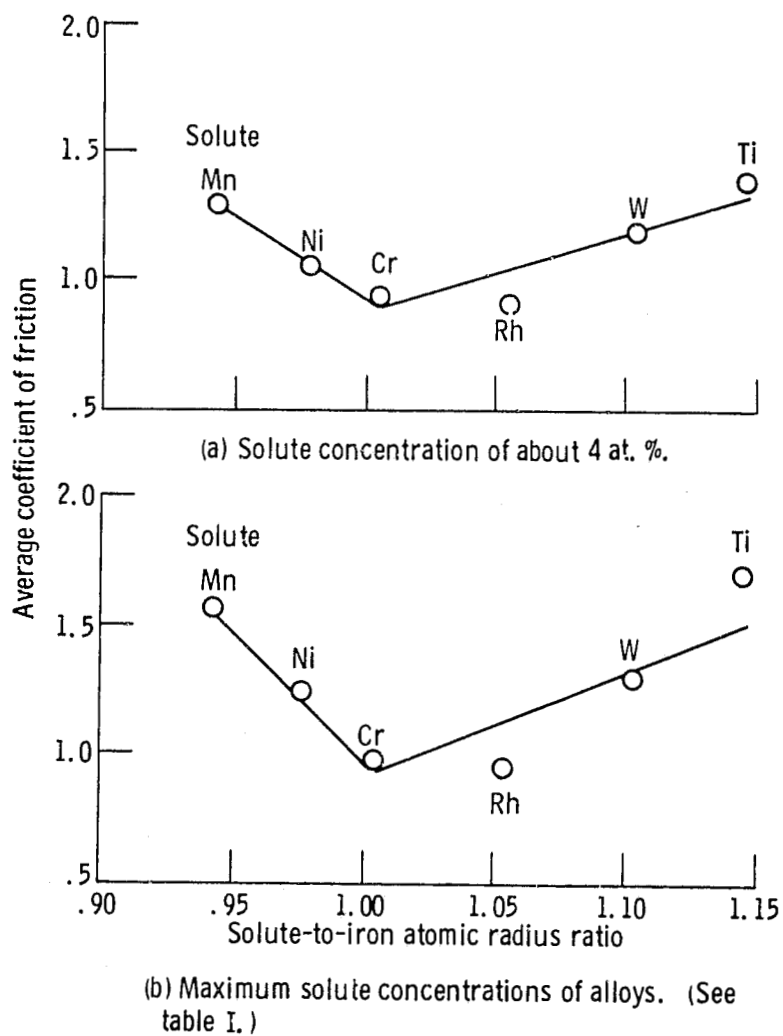
Figure 9. – Coefficients of friction for iron-based binary alloys as function of solute-to-iron atomic radius ratio. Single-pass sliding on single-crystal silicon carbide (0001) surface; sliding direction, $\langle 10\bar{1}0 \rangle$; sliding velocity, 3 mm/min; load, 0.2 N; room temperature; vacuum pressure, 10^{-8} Pa.
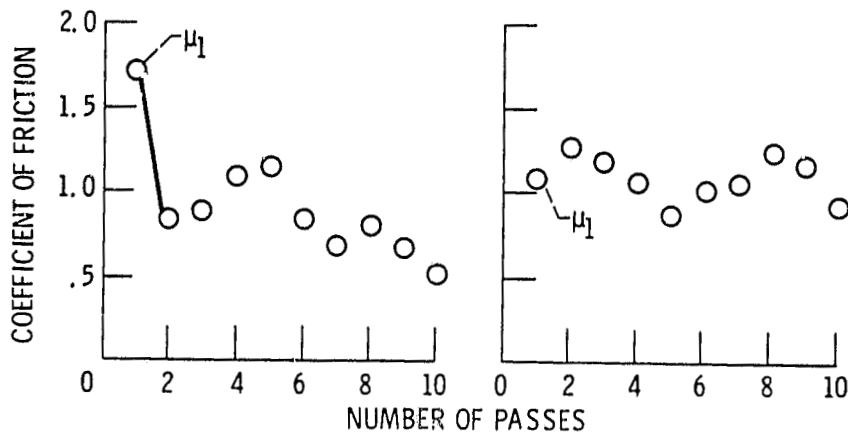
(a) 8.12 at. % Ti-Fe ALLOY.   (b) 8.06 at. % Rh-Fe ALLOY.

Figure 10. - Average coefficient of friction, calculated from maximum-peak-heights in friction trace, as function of number of passes of alloy riders across single-crystal silicon carbide (0001) surface. Load, 0.2 N.
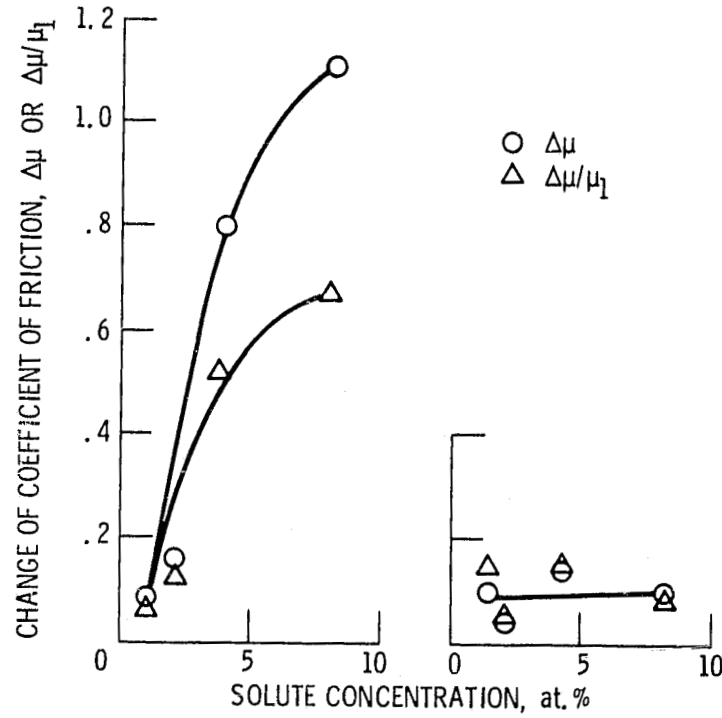
(a) Ti-Fe ALLOY.   (b) Rh-Fe ALLOY.

Figure 11. - Changes of coefficient of friction $\Delta\mu$ or $\Delta\mu/\mu_1$ with number of passes as a function of solute concentration.
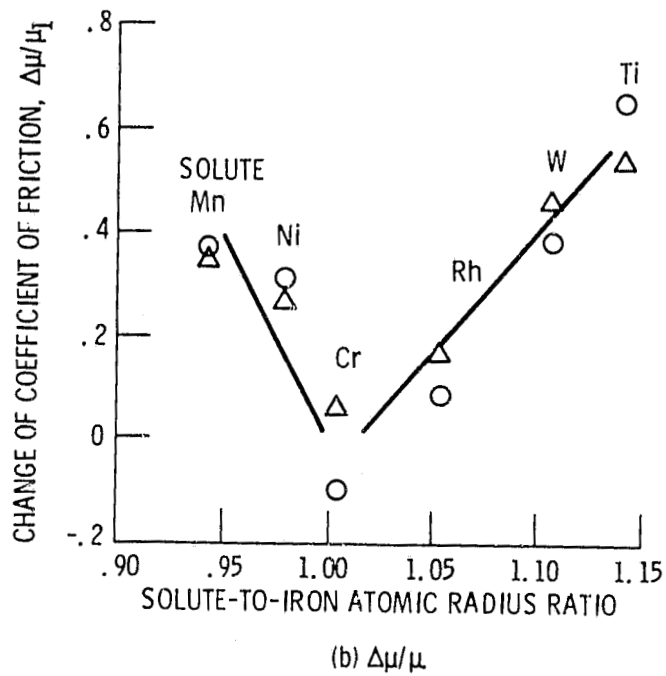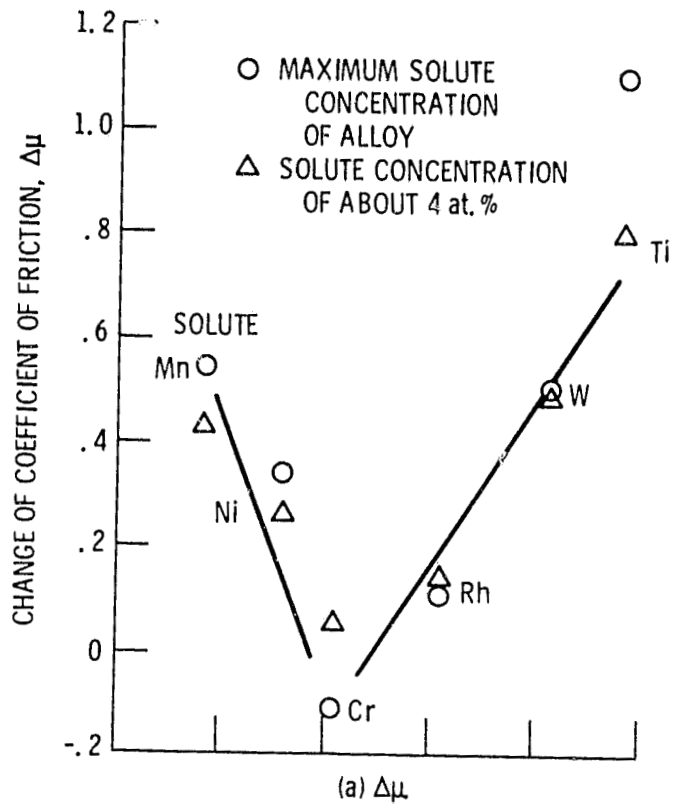
Figure 12. - Changes of coefficient of friction,
$\Delta\mu$ or $\Delta\mu/\mu_1$ as a function of solute-to-iron
atomic radius ratio.

1. Report No. NASA TM-79282	2. Government Accession No.	3. Recipient's Catalog No.
4. Title and Subtitle ADHESION, FRICTION, AND WEAR OF BINARY ALLOYS IN CONTACT WITH SINGLE-CRYSTAL SILICON CARBIDE		5. Report Date
		6. Performing Organization Code
7. Author(s) Kazuhisa Miyoshi and Donald H. Buckley		8. Performing Organization Report No. E-221
9. Performing Organization Name and Address National Aeronautics and Space Administration Lewis Research Center Cleveland, Ohio 44135		10. Work Unit No.
		11. Contract or Grant No.
12. Sponsoring Agency Name and Address National Aeronautics and Space Administration Washington, D.C. 20546		13. Type of Report and Period Covered Technical Memorandum
		14. Sponsoring Agency Code

15. Supplementary Notes

16. Abstract

Sliding friction experiments were conducted with various iron-base alloys (alloying elements were Ti, Cr, Mn, Ni, Rh and W) in contact with a single-crystal silicon carbide {0001} surface in vacuum. Results indicate atomic size misfit and concentration of alloying elements play a dominant role in controlling adhesion, friction, and wear properties of iron-base binary alloys. The controlling mechanism of the alloy properties is as an intrinsic effect involving the resistance to shear fracture of cohesive bonding in the alloy. The coefficient of friction generally increases with an increase in solute concentration. The coefficient of friction increases as the solute-to-iron atomic radius ratio increases or decreases from unity. Alloys having higher solute concentration produce more transfer to silicon carbide than do alloys having low solute concentrations. The chemical activity of the alloying element is also an important parameter in controlling adhesion and friction of alloys.

17. Key Words (Suggested by Author(s)) Silicon; Auger; Binary alloys; Adhesion; Friction	18. Distribution Statement Unclassified - unlimited STAR Category 27

19. Security Classif. (of this report) Unclassified	20. Security Classif. (of this page) Unclassified	21. No. of Pages	22. Price*